

## ROASTING TEMPERATURE EFFECT ON THE RECOVERY OF REFRACTORY GOLD AND SILVER IN PYRITE CONCENTRATES

Y.-P. Zhang <sup>a</sup>, K. Yang <sup>a</sup>, Y. Fang <sup>a</sup>, A. Robledo-Cabrera <sup>a</sup>, C.-S. Peng <sup>b,\*</sup>, A. Lopez-Valdivieso <sup>a,#</sup>

<sup>a</sup> Instituto de Metalurgia, Universidad Autónoma de San Luis Potosí, San Luis Potosí, Mexico

<sup>b</sup> School of Environmental and Chemical Engineering, Zhaoqing University, Zhaoqing, China

(Received 11 September 2020; Accepted 17 February 2021)

### Abstract

Pyrite concentrates with refractory gold and silver were roasted at different temperatures to improve the recovery of the metals by cyanide leaching. Scanning Electron Microscope characterization of the calcine revealed that the gold occluded in the pyrite less than one micron, and roasting produced channels in the concentrate, exposing the gold particles to the leaching solution. Gold and silver recoveries were maximum in the temperature range of 500-600°C due to the calcine high surface area and porosity. The Au and Ag recovery improved from 25 to 86% and 50 to 73%, respectively. The Au secondary encapsulation due to the sintering, the formation of the Ag-Fe-S species ( $Fe_{1-x}S + Ag_2S + Ag$ ) and Ag ferrite in higher roasting temperatures hence Au and Ag recoveries decreased.

**Keywords:** Gold recovery; Silver recovery; Roasting; Gold refractory; Cyanide leaching

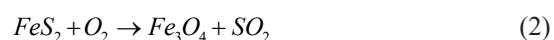
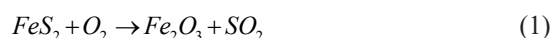
### 1. Introduction

Gold and silver in pyrite are not amenable to recovery by traditional cyanide leaching [1], because they are “refractory” since they are encapsulated (lock-up) in the sulfide minerals matrix [2] or as “invisible” particles — usually range from 50 to 200 Å — which cannot be detected even by high solution electron microscopes [3]. Besides, sulfide minerals consume oxygen and rob cyanide ions during the cyanidation, leading to insufficient cyanide ions and oxygen concentration for gold and silver leaching. The refractory minerals show a pretty poor gold and silver recovery rate (typically < 50%) [4]. Therefore, to improve the gold and silver recovery, the sulfide matrix structure should be cracked or dissolved to expose the gold and silver to the leaching reagent. To liberate gold and silver prior to cyanidation, processes such as roasting have been proposed.

Roasting is a promising option for sulfide pre-oxidation and has the advantages that are very fast and energetically self-supporting [5]. It was designed and developed in the early 20th century. Gidji Gold Processing plant, Australia, was the first commercial application of circulating fluidized-bed roasting to treat refractory sulfide ores with 1.2 g/t Au. The treatment capacity was 575 t/d and gold recovery was 80 to 85% [6]. The Syama goldfield, Mali, reported

Au reserves of 38.27 Mt with an average grade of 2.54 g/t Au. Through roasting a gold recovery of 85% was achieved [7]. In other plants such as Tongling in China and ETi Maden in Turkey, the throughput of gold sulfide ores are 1130 t/d and 630 t/d, respectively [8].

Oxidative roasting releases gold from refractory minerals by converting the iron to iron oxides and the sulfur to sulfur dioxide ( $SO_2$ ), besides, the latter reaction is used to produce sulfuric acid to prevent  $SO_2$  discharge and reduce environmental concerns [8-10]. In pyrite, it has been postulated that gold atoms in the metastable state migrate to a lower energetic site by solid-state diffusion [11]. Oxidation of pyrite is as follows (1-3):



The phases that are formed from pyrite oxidation at different temperatures (500, 600 and 700°C) are presented in Figure 1. At the lowest roasting temperature of 500°C, ferrous sulfate ( $FeSO_4$ ) and different iron oxides, such as hematite ( $\alpha$ - $Fe_2O_3$ ) and magnetite ( $Fe_3O_4$ ), formed as oxidized products.  $\alpha$ - $Fe_2O_3$  is the iron oxide terminal phase when

Corresponding author: [cspeng@ouc.edu.cn](mailto:cspeng@ouc.edu.cn) \*; [alopez@uaslp.mx](mailto:alopez@uaslp.mx) #;

<https://doi.org/10.2298/JMMB200911019Z>



increasing the temperature to 700°C.  $\alpha$ -Fe<sub>2</sub>O<sub>3</sub> is the ideal product for gold recovery since it is a highly porous matrix with good permeability and accessibility to gold particles. FeSO<sub>4</sub> and Fe<sub>3</sub>O<sub>4</sub> are intermediates and undesirable products as they are detrimental by higher cyanide consumption in leaching [1].

In general, converting pyrite to porous hematite by roasting to generate pores on the concentrate, making possible the contact between gold and leaching solutions. But the gold recovery has never been correlated to the specific surface area of the calcine. This work is aimed at further studying the effect of pyrite roasting temperature on the physical and chemical characteristics of the calcine and how these properties influence the gold and silver recovery. The pyrite and calcines were examined by Scanning Electron Microscope (SEM), X-ray diffraction (XRD) and chemical assay. The specific surface area and pore volume of calcines were determined to correlate to the gold and silver recovery by cyanide leaching.

## 2. Experimental

### 2.1. Materials and reagents

Two Au-pyrite concentrate samples from Chihuahua, México were used in this work. These concentrates were collected from the same gold-pyrite

ore; therefore, they have the same mineralogy, the only difference was in the grade of the element components. Scanning Electron Microscope (SEM) reported that pyrite (FeS<sub>2</sub>), chalcopyrite (CuFeS<sub>2</sub>), galena (PbS), and sphalerite (ZnS) were contained in the concentrates. Calculation based on the elemental chemical assays (Table 1) revealed that sample 1 contained 82.3% FeS<sub>2</sub>, 0.2% CuFeS<sub>2</sub>, 0.4% PbS, and 0.7% ZnS, and sample 2 contained 88.9% FeS<sub>2</sub>, 0.4% CuFeS<sub>2</sub>, 1.4% PbS, and 2.7% ZnS. X-ray Diffraction (XRD) also confirmed that FeS<sub>2</sub> was the main sulfide mineral in the concentrates (Figure 2). The particle size distribution of the two samples was similar. It was determined by wet sieving through different size meshes and shown in Figure 3. The sample size was 80% passing 150  $\mu$ m. The sodium cyanide used in the gold and silver leaching tests was from J.T.Baker. All leaching tests were carried out using tap water and lime for pH adjustment.

SEM characterization revealed that gold in the Au-FeS<sub>2</sub> concentrates existed as native Au, and electrum (Au-Ag), less than 2  $\mu$ m in size. Most of the Au was occluded in the FeS<sub>2</sub> grains and only about 25% of it was exposed to cyanide leaching solutions. As for silver, this metal value was acanthite (Ag<sub>2</sub>S), hessite (Ag<sub>2</sub>Te), and eckerite (Ag<sub>2</sub>CuAsS<sub>3</sub>). Figure 4 shows the gold and silver minerals in the concentrates.

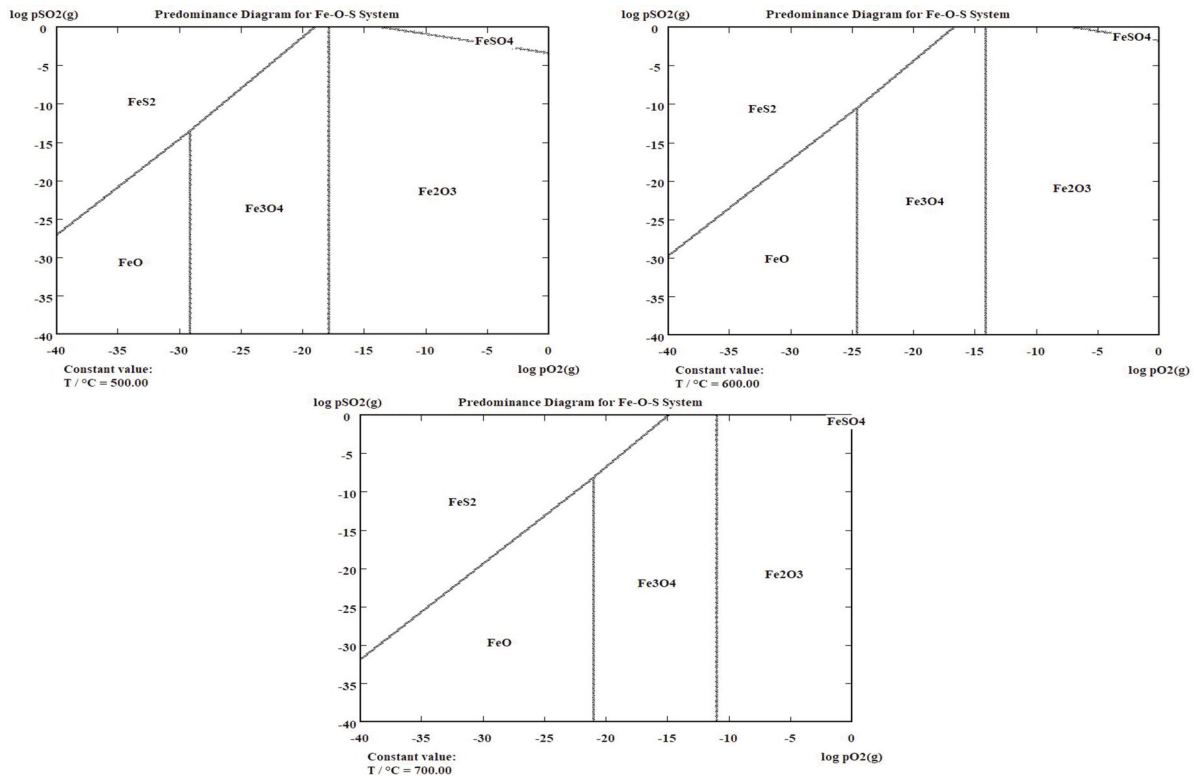


Figure 1. Stability phase diagram of pyrite roasting at 500, 600, and 700°C, built using the (HSC) chemistry 6 software



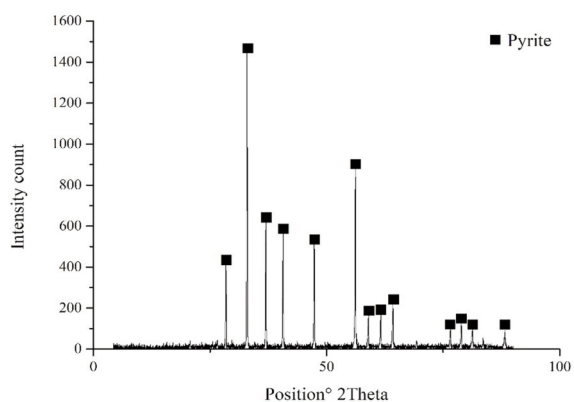


Figure 2. XRD of pyrite concentrate

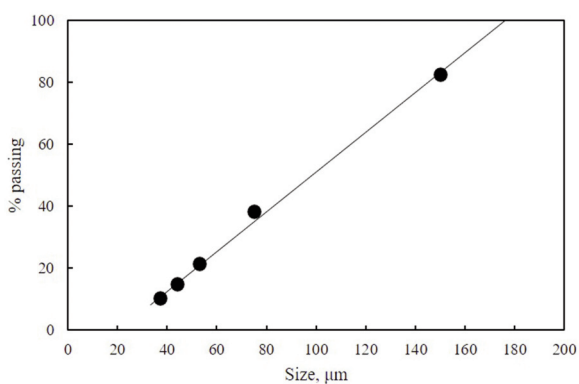


Figure 3. The particle size distribution of Au-pyrite concentrate

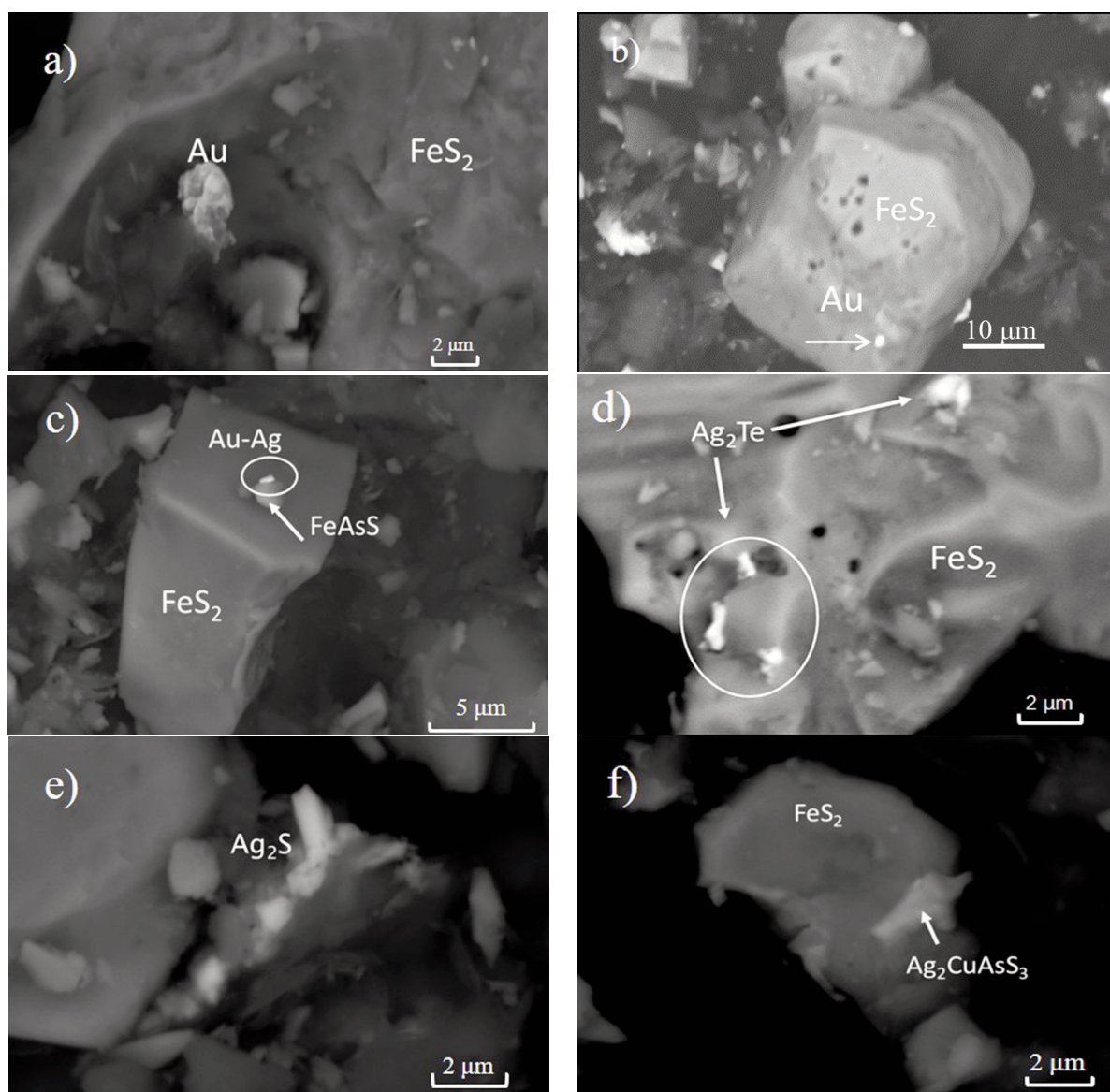


Figure 4. SEM photomicrograph of gold and silver minerals in Au-pyrite concentrate. Native Au, Electrum (Au-Ag), Acanthite ( $Ag_2S$ ), Hessite ( $Ag_2Te$ ) and Eckerite ( $Ag_2CuAsS_3$ )

## 2.2. Roasting

Roasting of the pyrite concentrate was carried out in a tube furnace. 35g pyrite was uniformly placed in a ceramic container, which was placed into an alumina tube once the temperature achieved the desired value. Roasting tests were performed in the temperature range of 400 to 700°C, and in the time range of 4-6 h. Air was injected into the tube at a flow rate of 10 mL min<sup>-1</sup>. Outgas from the furnace was directed to a bucket with a sodium hydroxide solution to trap the SO<sub>2</sub>. Pre-oxidation was completed until SO<sub>2</sub> stopped emanating which was detected by no pH changes in the sodium hydroxide solution. The calcine was characterized by gold and silver content, surface area, SEM and XRD. Au and Ag recovery from the calcine was determined by cyanide leaching.

## 2.3. Cyanidation

Cyanidation tests were performed in a 250 mL glass stirring reactor using a 200 mL cyanide solution (concentration was 1,000 mg/L) and 30 g calcine (15%w solid slurry). The slurry pH was adjusted to 10.5-11 and maintained constant throughout the leaching test. Air was continuously injected into the slurry during the leaching test. The O<sub>2</sub> concentration in the slurry was 7.2 ppm throughout the test. The O<sub>2</sub> concentration in the slurry was 7.2 ppm throughout the leaching tests and was measured by a dissolved oxygen meter equipped with an electrode (ST 300D, OHAUS). This oxygen concentration was consistent with the saturation concentration of dissolved oxygen in water at the temperature range of 20-30°C [21]. The leaching time was 72 h. Afterward, the solid was

filtered, dried and prepared for Au and Ag assay. Au and Ag in original samples, leaching aqueous solutions and residues were analyzed by Atomic Absorption Spectroscopy (AAS).

## 2.4. Equipments

XRD was carried out with an X-ray diffractometer (D8Advance Bruker). The SEM used was a JSM-6610LV, JEOL. The Atomic Absorption Spectrophotometer for the chemical analysis of samples was Perkin Elmer 3110. To determine the specific surface area and porosity of samples a physisorption equipment (Autosorb-1, Quantachrome) was used. Nitrogen was the adsorbent for the measurement of the surface area. The Brunauer Emmett Teller (BET) model and the density functional theory (DFT) method were used for calculating the surface area and porosity of samples.

## 3. Results and discussion

### 3.1. Roasting Temperature and Time

Figure 5 shows the XRD diffractogram of the pyrite concentrate and the calcines after roasting at 400, 450, 500, 600, and 700°C, and time (4 and 6 h). The XRD diffractogram revealed that maghemite ( $\gamma$ -Fe<sub>2</sub>O<sub>3</sub>) and magnetite (Fe<sub>3</sub>O<sub>4</sub>) appeared as the final pyrite oxidation at 450°C and 6 h, while at 400°C no iron oxides were detected meaning very mild pyrite oxidation and longer time was needed for the oxidation process.  $\gamma$ -Fe<sub>2</sub>O<sub>3</sub> is a metastable spinel polymorph of hematite ( $\alpha$ -Fe<sub>2</sub>O<sub>3</sub>) and an intermediate product from magnetite to hematite. It was reported that maghemite rendered the mineral refractory and

Table 1. Chemical composition of Au-pyrite concentrates

Original sample	Amount %					g/t		
	Cu	Pb	Zn	Fe	S	Insoluble	Au	Ag
1	0.07	0.35	0.46	38.5	48	5.7	18.2	238
2	0.14	1.2	1.8	41.5	48	6.6	14.8	366

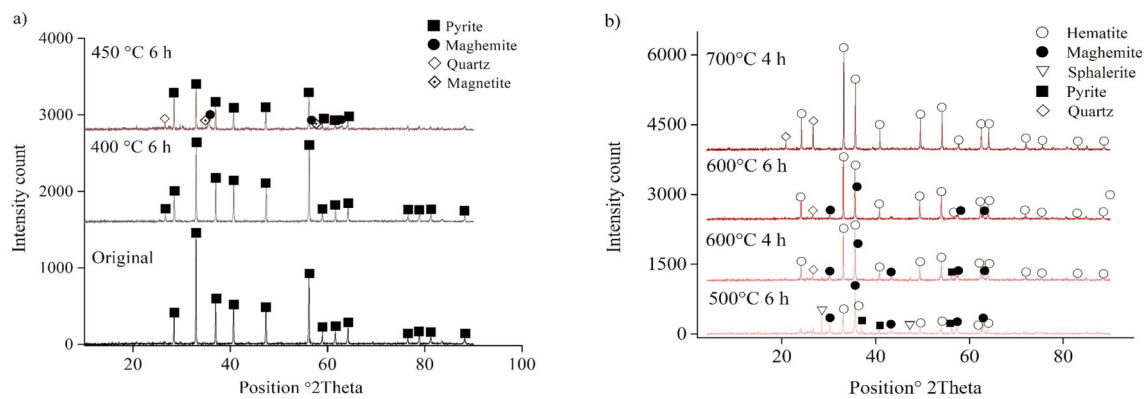


Figure 5. XRD of a) original sample and sample roasted at 400 and 450°C; b) roasted sample at 500-700°C



made a tough gold recovery by cyanidation [13]. The formation of the  $\alpha\text{-Fe}_2\text{O}_3$  was present in the roasting temperature up to  $500^\circ\text{C}$ , while pyrite oxidation was still not completed during 6 h roasting, neither at  $600^\circ\text{C}$ , 4 h. Then pyrite was completely converted to iron oxides when the roasting time increased to 6 h at  $600^\circ\text{C}$  and higher temperature. At  $700^\circ\text{C}$ , only  $\alpha\text{-Fe}_2\text{O}_3$  was detected in the calcine.

Figure 6 shows SEM photomicrographs of the pyrite sample and calcines at the various roasting temperatures. As noted, a thin layer of iron oxides ( $\gamma\text{-Fe}_2\text{O}_3$  and  $\text{Fe}_3\text{O}_4$ ) formed on the edge of the pyrite particle at  $450^\circ\text{C}$  (Figure 6 a-b), which confirmed the species by results in Figure 5 (a). It can be seen that  $\text{Fe}_3\text{O}_4$  was first formed around the pyrite, then the

$\text{Fe}_3\text{O}_4$  was oxidized to  $\gamma\text{-Fe}_2\text{O}_3$  and  $\alpha\text{-Fe}_2\text{O}_3$  when the roasting temperature increased. At  $500^\circ\text{C}$  (Figure 6 c-d),  $\alpha\text{-Fe}_2\text{O}_3$  appeared at the particle edge where there were  $\text{Fe}_3\text{O}_4$ ,  $\gamma\text{-Fe}_2\text{O}_3$ , and iron sulfate ( $\text{FeSO}_4$ ) as predicted by the diagram shown in Figure 1. The formation of these iron oxides was confirmed by other studies, which reported that  $\gamma\text{-Fe}_2\text{O}_3$  was an intermediate product during pyrite oxidation and  $\alpha\text{-Fe}_2\text{O}_3$  was the final product [12, 14, 15]. Moreover,  $\alpha\text{-Fe}_2\text{O}_3$  was the only iron oxide at the roasting temperature of  $700^\circ\text{C}$  (Figure 6 e-f). In this study, we chose  $500\text{-}700^\circ\text{C}$  to recovery gold and silver as the calcine presented distinct iron oxide phases and the aim was to delineate how this affected the metal recoveries.

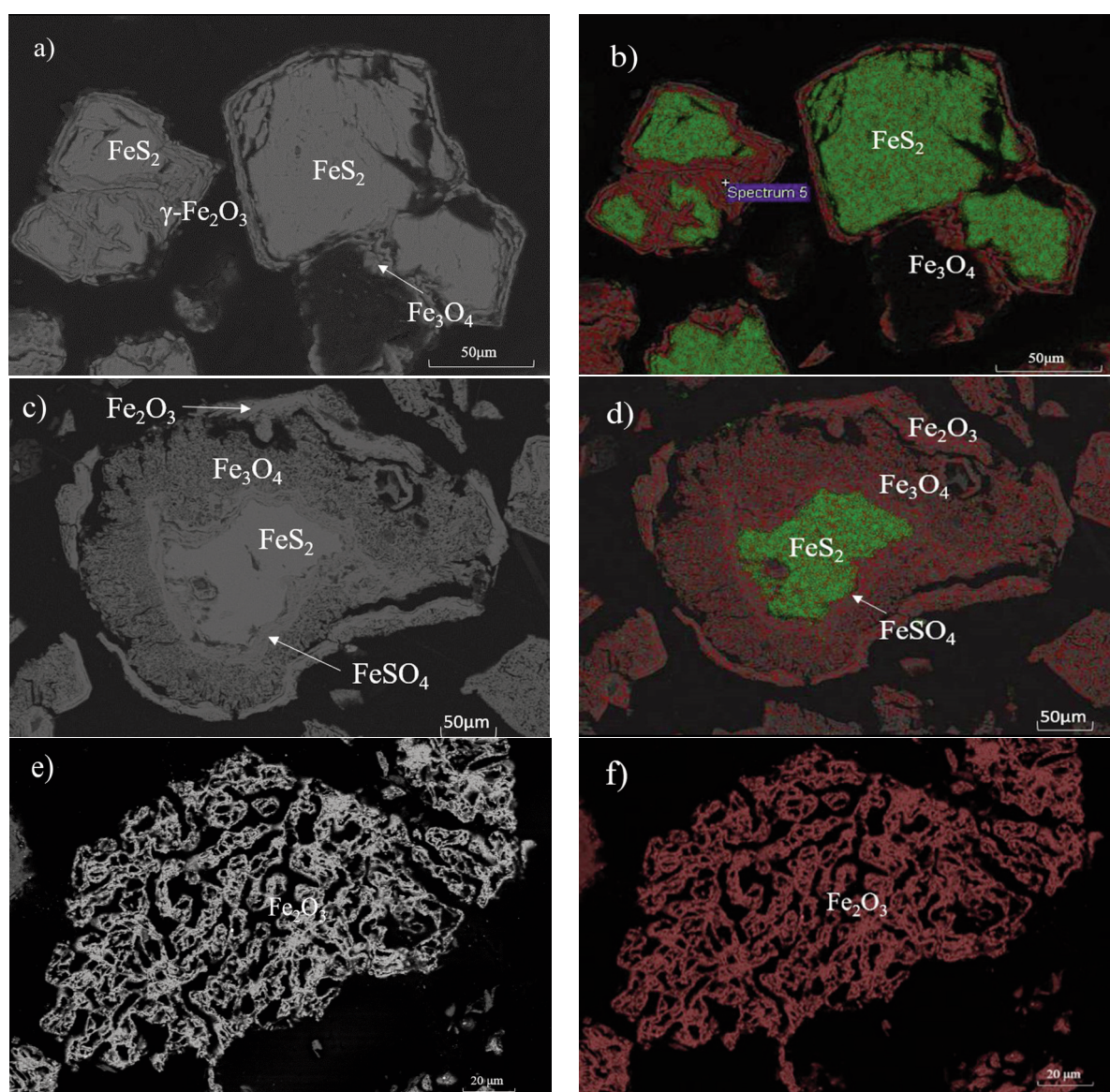


Figure 6. SEM photomicrographs of pyrite oxidized at: a-b)  $450^\circ\text{C}$ , c-d)  $500^\circ\text{C}$  and e-f)  $700^\circ\text{C}$ ; b, d and f are the elemental mapping, red color dots represent Fe and green color dots represent S

Most roasting processes of pyrite are carried out at 700°C, achieved from the heat evolved during the highly exothermic oxidation of pyrite [8]. However, sintering was reported to occur under these conditions [17, 18]. The specific surface area and porosity of the original samples and calcines are presented in Table 2 and Figure 7. Compared to the original sample, the surface area and pore volume of the roasted products, especially the meso and micro-porosity, increased one order of magnitude when roasting was carried out at 500 and 600°C. But the surface area and porosity significantly decreased when the temperature increased up to 700°C, meaning that particles sintering occurred during roasting.

### 3.2. Chemical Analysis of Calcines

The mass loss of the original sample and a chemical assay of the calcines are given in Table 3. Increasing the temperature up to 500-700°C, the mass loss increased linearly, which confirmed that the S in the pyrite was oxidized to SO<sub>2</sub> gas during the roasting. The S content was reduced significantly from 48% to 11% at 500°C, and only 1.9% S remained in the calcine when the roasting was at 600°C for 6 h. Due to the different types of original samples, there was still 3.7% S of the product at 700°C for sample 2. XRD and SEM showed that iron oxides formed during roasting. As a consequence of the mass loss, the grade of Fe, Au, and Ag in the calcine more than the original samples. The Au grade increased from 18.2 g/t to 36-30 g/t, supposedly it would be easier to recover by leaching solution [12, 17, 19].

Figure 8 shows SEM photomicrographs of roasted samples (500-700°C) where a random porous structure can be observed. Besides, it is seen that more

fine gold and silver particles were exposed which is beneficial for recovery. The size of the gold and silver particles was about one micron and there were particles with an even smaller size. The porous structure of the calcine would definitely allow cyanide solution and oxygen to migrate to the gold and silver particles and dissolve them.

### 3.3. Au and Ag cyanide leaching from calcines

The calcines from the pyrite-sample roasting were treated to cyanide leaching to extract the gold and silver. After roasting, the sample was ground to 0.25 mm and cyanide leached at pH 10.5-11 for 72 h. The gold and silver recovery are presented in Figure 9. The original sample exhibited very poor gold recovery (25%) and Ag recovery (50%) because they were occluded in the pyrite grains. A higher gold recovery of the order of 85% was achieved at 500 and 600°C. Under these conditions, high porosity was

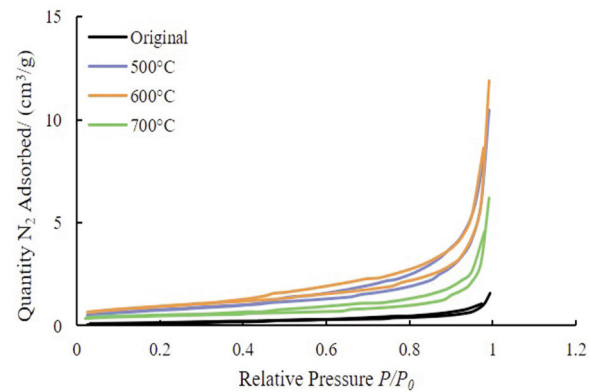


Figure 7. Nitrogen adsorption isotherms of calcines from roasting pyrite at 500, 600 and 700°C

Table 2. Specific surface area and pore volume of the original and roasted samples at 500, 600 and 700°C

Sample	Surface area (m <sup>2</sup> /g)	Porosity volume (cc/g)	Micro-pore		Meso-pore		Macro-pore	
			Volume (cc/g) x10 <sup>-3</sup>	%	Volume (cc/g) x10 <sup>-3</sup>	%	Volume (cc/g) x10 <sup>-3</sup>	%
Original	0.55	0.001	0	0	2.14	21	2.12	79
500°C	2.76	0.009	0.62	21	1	33	0.14	46
600°C	3.31	0.1	1.05	30	0.13	36	0.12	34
700°C	1.68	0.005	0.8	33	0.51	21	0.16	67

Table 3. Weight loss and chemical analysis of original and calcines samples

Time, h	Temp. °C	Weight Loss, %	Chemical Assay							
			%						g/t	
			Cu	Pb	Zn	Fe	% S	Ins.%	Au	Ag
Sample 1	-	-	0.07	0.35	0.46	38.5	48	5.72	18.2	238
6	500	22	0.07	0.39	0.69	51.5	11	9.62	26.8	278
4	600	28	0.08	0.44	0.78	56	4.3	10	31	291
6	600	29	0.08	0.42	0.75	56	1.9	10	28.5	299
Sample 2	-	-	0.14	1.2	1.8	41.5	48	-	14.8	366
4	700	38.3	0.19	1.51	2.11	50.4	3.7	-	20.8	381



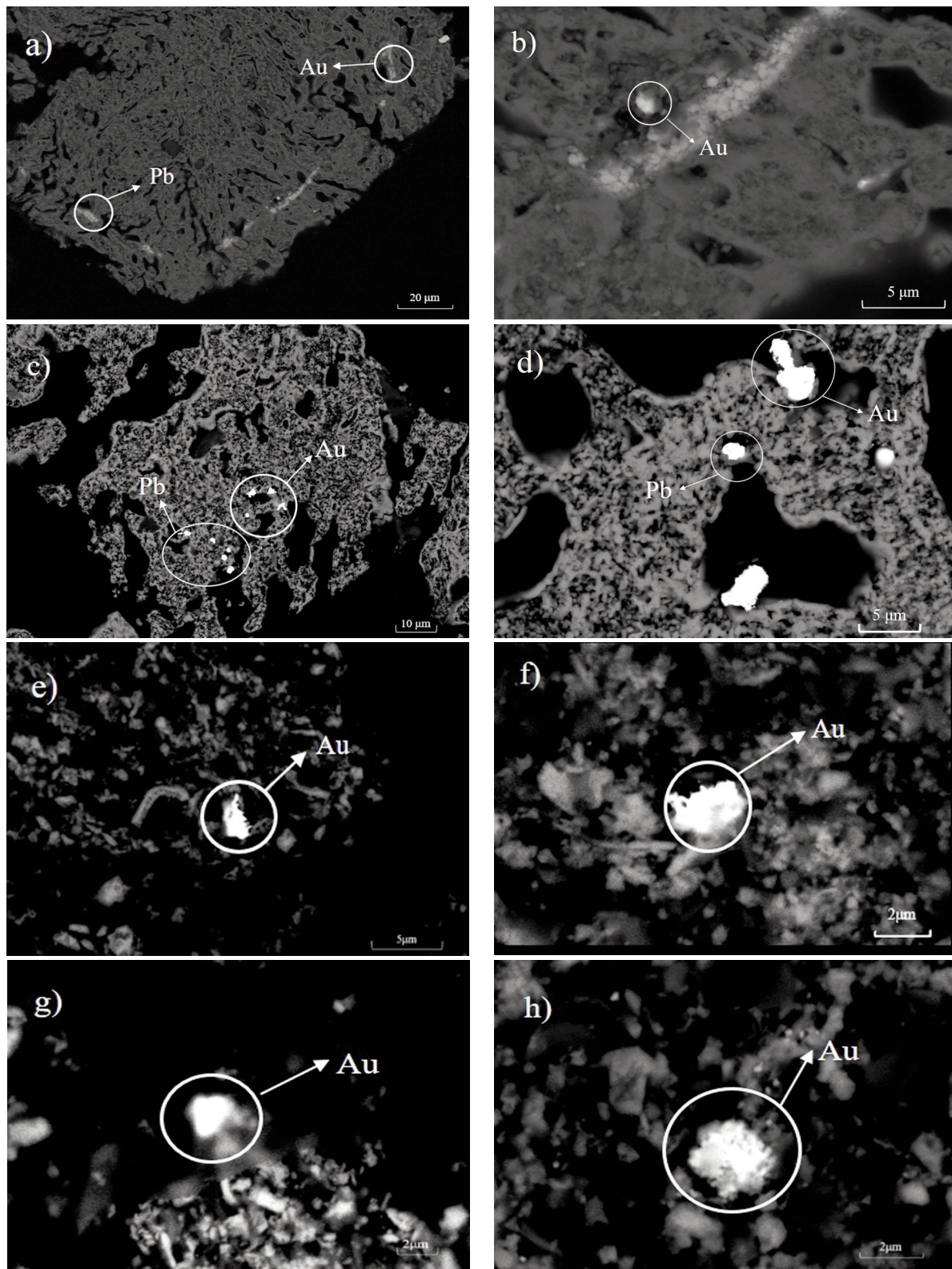


**Figure 8.** SEM photomicrographs of roasted samples: (a-b) 500°C, 6 hrs; (c-d) 600°C 4 hrs; (e-f) 600°C, 6 hrs; (g-h) 700°C 4 hrs. The porous matrix is iron oxide hematite and the white and shining phases marked by an open circle are gold. The shining phases without open circles are lead minerals

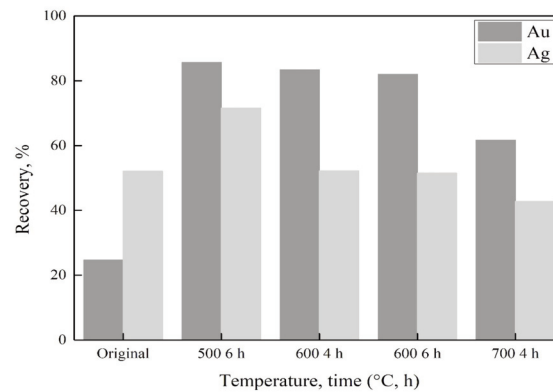
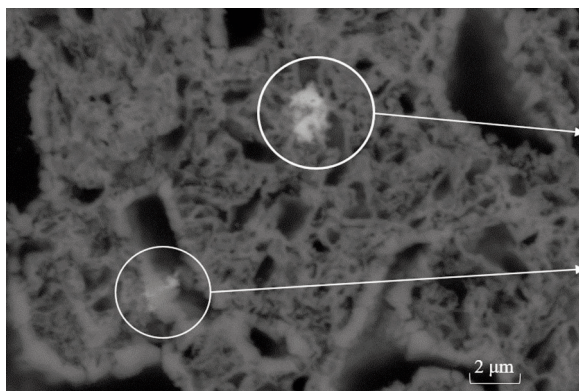


**Figure 9.** Recovery of gold and silver from original and roasted Au-pyrite concentrate at various roasting temperatures and times



Element	Weight %	Atomic %
O	27.02	62.24
S	6.56	7.54
Fe	23.65	15.61
Ag	42.76	14.61
Element	Weight %	Atomic %
O	30.67	62.25
S	2.02	2.05
Fe	55.04	32.01
Ag	12.26	3.69

**Figure 10.** SEM photomicrograph of residues after cyanide leaching of calcine obtained by roasting 600°C, 6 h. The white circle indicates the element composition of the phase by EDS

attained in the calcine exposing more gold to the cyanide leaching solution. When the roasting temperature increased to 700°C, gold recovery decreased significantly to 43%. Comparing the gold recovery with the calcine specific surface area, it is noted that this lowering in gold recovery is associated with a decrease in the calcine surface area due to the sintering of the iron oxides. As a consequence, gold particles were encapsulated in the iron oxides and no longer accessible to oxygen and cyanide solution. This phenomenon is known as secondary gold physical encapsulation [16].

Silver recovery reached 73% at 500°, an increase of 23% when compared with the 50% recovery for the original sample. This silver recovery lowered when roasting temperature increased above 500°C, which may be due to the formation of the Ag-Fe-S eutectic compound with low solubility in cyanide solutions. According to Raghavan [20], the Ag-Fe-S species ( $\text{Fe}_{1-x}\text{S} + \text{Ag}_2\text{S} + \text{Ag}$ ) formed through a ternary eutectic reaction at 532°C. A silver species linked to Fe and S was detected in the calcine by SEM-EDS as shown in Figure 10, On the other hand, the formation of silver ferrite during the roasting process is another possible reason for the decrease in Ag recovery [19].

#### 4. Conclusions

Direct cyanidation on Au-pyrite concentrates only recovers less than 25% Au and 55% Ag, because of their high refractoriness. Therefore, the pyrite concentrate needed to be pre-treated to liberate gold and silver particles. Au and Ag recovery improved significantly after roasting, which converted the pyrite to maghemite, iron sulfate, and hematite. An Au recovery of over 85% was attained at 500 to 600°C due to the high porosity of the calcine exposing occluded ultrafine gold to leaching solutions. Above 600°C, hematite sintered in the calcine giving rise to a decrease in Au recovery. Secondary gold encapsulation occurred under these conditions. Ag recovery increased when the roasting temperature was 500°C, then declined at temperatures above 600°C not only because of encapsulation but due to the formation of Ag-Fe-S species, which are not dissolved by cyanide.

#### Acknowledgments

Yipeng Zhang, Ke Yang and Yi Fang acknowledge the National Council for Science and Technology, Mexico (CONACyT) for the fellowship 900333,





900347 and 900339, respectively, to pursue Ph.D. studies in Materials Science and Engineering at the Universidad Autónoma de San Luis Potosí, México. Financial support from Minera Río Tinto, Chihuahua, México to carry out this work is fully acknowledged.

## References

- [1] T. Chen, L. Cabri, J. Dutrizac, JOM., 54 (12) (2002) 20-22.
- [2] B. Xu, Y.B. Yang, Q. Lian, G.H. Li, T. Jiang, Hydrometallurgy, 147-148 (2014) 79-82.
- [3] M. Hochella, B.M. Bakken, A.F. Marshall, Process mineralogy., Metallurgical Society of American, Warrendale, Pennsylvania, 1988, p. 153-155.
- [4] S. Faraz, A. Hossna, B. Rezag, Z. Piroz, Int. J. Min. Sci. Technol., 24 (4) (2014) 537-542.
- [5] J.G. Dunn, A.S. Ibrado, J. Graham, Miner. Eng., 8 (4-5) (1995) 459-471.
- [6] J. Marsden, L. House, The chemistry of gold extraction, Ellis Horwood Ltd, England, 2006, p. 14-16
- [7] I. Ballo, K. Hein, B. Guido, L. Sanogo, Y. Ouologuem, G. Daou, A. Traore. Ore. Geol. Rev., 78 (2016) 578-585.
- [8] M. Runkel, P. Sturm. J. South., Afr. Inst. Min. Metall., 109 (8) (2009) 491-496.
- [9] C. Yang, Y. Chen, P. Peng, C. Li, X. Chang, Y. Wu, J. Hazard. Mater., 167 (1) (2009) 835-845.
- [10] Y. Liu, B. Zhao, Y. Tang, P. Wan, Y. Chen, Z. Lv, Thermochem. Acta., 588 (2014) 11-15.
- [11] A. Filmer, J. South. Afr. Inst. Min. Metall., 82 (3) (1982) 90-94.
- [12] D. Paktunc, D. Kingston, A. Pratt, J. McMullen, Can. Mineral., 44 (1) (2006) 213-227.
- [13] A. Bas, W. Zhang, E. Ghali, Y. Choi, Hydrometallurgy, 158 (2015) 1-9.
- [14] S. Music, S. Popovic, M. Ristic. J. Radioanal. Nucl. Chem., 162 (2) (1992) 217-226.
- [15] X. Liu, J. Shaw, J. Jiang, J. Bloemendal, P. Hesse, T. Rolph, X. Mao, Sci. China. Earth. Sci., 53 (8) (2010) 1153-1162.
- [16] Y. Zhang, Q. Li, X.L. Liu, B. Xu, Y.B. Yang, T. Jiang, Minerals, 9 (4) (2019) 220-222.
- [17] J. Hammerschmidt, J. Güntner, B. Kerstiens, A. Charitos, Gold ore processing (second edition). Elsevier, Amsterdam, 2016, p. 393-409.
- [18] X. Liu, Q. Li, Y. Zhang, T. Jiang, Y. Yang, B. Xu, Y. He, Metall. Mater. Trans. B., 50 (4) (2019) 1588-1596.
- [19] F. Espiell, A. Roca, M. Cruells, C. Niji, Hydrometallurgy, 16 (2) (1986) 141-151.
- [20] V. Raghavan, J. Phase. Equilibria. Diffus. 25 (3) (2004) 272.
- [21] H. Patel, and Vashi, R.T. Characterization of Textile Wastewater, Elsevier, Amsterdam, 2015, p. 21-71.

## UTICAJ TEMPERATURE PRŽENJA NA ISKORIŠĆENJE REFRAKTORNOG ZLATA I SREBRA IZ KONCENTRATA PIRITA

Y.-P. Zhang <sup>a</sup>, K. Yang <sup>a</sup>, Y. Fang <sup>a</sup>, A. Robledo-Cabrera <sup>a</sup>, C.-S. Peng <sup>b,\*</sup>, A. Lopez-Valdivieso <sup>a,#</sup>

<sup>a</sup> Institut za metalurgiju, Univerzitet de San Luis Potosí, San Luis Potosí, Meksiko

<sup>b</sup> Fakultet za hemijsko inženjerstvo i zaštitu životne sredine, Univerzitet Žaoćing, Žaoćing, Kina

### Apstrakt

Koncentrat pirita sa refraktornim zlatom i srebrom pržen je na različitim temperaturama da bi se poboljšalo iskorišćenje metala pri luženju cijanidom. Karakterizacija kalcinata skenirajućim elektronskim mikroskopom otkrila je da je zlato okludiralo u piritu manje od jednog mikrona, i da je prženje stvorilo kanale u koncentratu izlažući čestice zlata rastvoru za luženje. Iskorišćenje zlata i srebra je bilo najveće na temperaturama u rasponu od 500-600°C zbog velike površine i poroznosti kalcinata. Iskorišćenje Au i Ag je poraslo sa 25 na 86% i sa 50 na 73%, pojedinačno. Iskorišćenje Au i Ag je bilo smanjeno zbog sekundarne enkapsulacije Au usled sinterovanja, formiranja Ag-Fe-S jedinjenja ( $Fe_{1-x}S + Ag_2S + Ag$ ) i Ag ferita na višim temperaturama prženja.

**Ključne reči:** Iskorišćenje zlata; Iskorišćenje srebra; Prženje; Refraktorne zlato; Luženje cijanidom

